0026-895X/95/010104-11$03.00/0

MOLECULAR PHARMACOLOGY, 47:104–114, 1995.

ADP and ATP Activate Distinct Signaling Pathways in Human Promonocytic U-937 Cells Differentiated with 1,25-Dihydroxy-vitamin D_3

M. ANGELES VENTURA and PIERRE THOMOPOULOS

U-282 INSERM, Hôpital Henri Mondor, 94010 Créteil, France (M.A.V.), and Department of Endocrinology, Hôpital Cochin, 75014 Paris, France (P.T.)

Received April 4, 1994; Accepted October 28, 1994

SUMMARY

We investigated the effects of purinergic P_2 agonists on cell adhesion, as well as the signaling pathways involved, in U-937 human promonocytic cells differentiated to a more mature monocytic phenotype with 1,25-$(OH)_2$-vitamin D_3. In cell adhesion studies, ATP was more potent than ADP, whereas ADP showed greater efficacy. The time course of the intracellular calcium concentration ($[Ca^{2+}]_i$) response to ATP was biphasic (a spike followed by a plateau), whereas ADP evoked a plateau after a time lag of several seconds. The spike $[Ca^{2+}]_i$ response evoked by ATP was due to both *myo*-inositol-1,4,5-trisphosphate-induced Ca^{2+} mobilization and influx, whereas the ADP effect was Ca^{2+} influx dependent. Moreover, ADP and ATP activated distinct Ca^{2+} influx mechanisms, as shown by Mn^{2+} quenching of the fura-2 signal, which was slow and long-lasting for ADP but rapid for ATP. Treatment with phorbol dibutyrate shifted the EC_{50} of the $[Ca^{2+}]_i$ spike response to the right and abolished the plateau response. Accordingly, phorbol dibutyrate inhibited the ADP-evoked response but only partly inhibited the ATP-evoked Ca^{2+} influx. cAMP-raising agents had no effect on the $[Ca^{2+}]_i$ spike or on Ca^{2+} influx but delayed or transiently inhibited the plateau phase. The plateau response thus appears to be independent of the spike response, because it can be directly evoked by ADP and undergoes distinct regulation. This suggests that ADP and ATP activate U-937 cells through distinct signaling pathways, probably involving specific receptors.

ATP and ADP act as intercellular signaling molecules for cells of virtually all origins (1, 2). They are released from the cytoplasm of several cell types and by exocytosis from nerve terminals and platelets (3). ATP and ADP interact with specific receptors termed P_2 receptors, whereas their dephosphorylation product adenosine interacts with P_1 receptors (3). Several subtypes of P_2 purinergic receptors have been described on the grounds of functional responses and agonist potency, because no specific antagonists are available (3–5). The P_{2Z} subtype opens a pore (6) and the P_{2X} subtype a Ca^{2+} channel (7) in the plasma membrane; the P_{2Y} subtype activates phospholipase C (1) and the P_{2T} subtype activates both a Ca^{2+} channel and a phospholipase C (8). The "nucleotidic" or P_{2U} subtype shares the mechanism of action of the P_{2Y} subtype but shows a distinct pattern of agonist potency (4). A P_{2U} subtype from mouse neuroblastoma (9) and a P_{2Y} variant from chicken brain (10) have recently been cloned.

Blood cells, such as platelets, lymphocytes, and neutrophils, are targets for purinergic agonists (3, 11). The P_{2U} receptor of human neutrophils and their precursor cell line HL-60 has been extensively studied for its biological effects, pharmacology, and signaling pathways (2, 12). ATP binding results in the activation of a phospholipase C coupled to a pertussis toxin-sensitive G protein (13). This is also true of murine macrophages, i.e., both peritoneal macrophages (14) and the cell line J774 (15). Less is known about the purinergic receptor(s) of monocytes. Platelet-released ATP and ADP stimulate the phagocytic activity of neutrophils and monocytes (12) and ADP increases the binding of fibrinogen to monocytes in a Ca^{2+}-dependent reaction (16). ADP and ATP have been reported to increase $[Ca^{2+}]_i$ in human monocytes (2) and U-937 cells (2, 17, 18).

Circulating monocytes are a source of inflammatory agents, play a role in hemostasis, participate in defense mechanisms such as antigen presentation and phagocytosis, and are involved in atherogenesis as scavenging agents (19). When activated by appropriate stimuli, they adhere to, and then cross, the endothelium, thereby becoming tissue macrophages. We have shown that the adhesiveness of the promonocytic cell line U-937 is increased by activators of phospholipase C and is inhibited by cAMP-raising agents such as β-adrenergic receptor agonists,

ABBREVIATIONS: $[Ca^{2+}]_i$, cytosolic free Ca^{2+} concentration; IP_3, *myo*-inositol-1,4,5-trisphosphate; AMP-PCP, adenylyl (β,γ-methylene)-diphosphonate; ATPγS, adenosine-5′-*O*-(3-thio)triphosphate; ADPβS, adenosine-5′-*O*-(2-thio)diphosphate; 2-Me-S-ATP, 2-methylthio-ATP; 2-Me-S-ADP, 2-methylthio-ADP; 2A5P, P^1,P^5-di(adenosine-5′)pentaphosphate; PGE_1, prostaglandin E_1; PDBu, phorbol-12,13-dibutyrate; PAF, platelet-activating factor; PI3K, phosphatidylinositol 3-kinase; PDGF, platelet-derived growth factor; HEPES, 4-(2-hydroxyethyl)-1-piperazineethanesulfonic acid; EGTA, ethylene glycol bis(β-aminoethyl ether)-*N*,*N*,*N*′,*N*′-tetraacetic acid; ANOVA, analysis of variance; LSD, least significant difference.

prostaglandins, and adenosine (20). Preliminary studies indicate that ATP stimulates U-937 cell adhesiveness (21). Because P_1 (adenosine) and P_2 (ATP) purinergic receptors play opposite roles in these cells, purinergic signaling might constitute a regulatory feedback mechanism.

We investigated P_2 purinergic effects on U-937 cells and found that in adhesion studies ATP was more potent, whereas ADP showed greater efficacy. Specific patterns of $[Ca^{2+}]_i$ responses to ADP and ATP were identified. Moreover, the $[Ca^{2+}]_i$ response evoked by ATP was due to both Ca^{2+} mobilization and influx, whereas the ADP effect relied on Ca^{2+} influx. These results suggest that ADP and ATP activate distinct signaling pathways, probably involving specific receptors.

Materials and Methods

Reagents. RPMI 1640 medium and fetal and newborn calf sera were from Eurobio (Montrouge, France), fluo-3 and $[Ca^{2+}]$ standards from Molecular Probes (Eugene, OR), AMP-PCP and ATPγS from Boehringer Mannheim (Meylan, France), and 2-Me-S-ADP and 2-Me-S-ATP from Research Biochemicals (Natick, MA). 1,25-$(OH)_2$-cholecalciferol and Ro-20174 were kindly provided by Dr. U. Fisher, Hoffmann-La Roche (Basel, Switzerland), and SKF-96365 by Dr. T. Merritt, SmithKline Beecham (The Frythe, UK). [*methyl*-^{3}H]Thymidine (specific activity, 70–85 Ci-mmol) and the [^{3}H]IP_3 assay system were from Amersham (Bucks, UK). All other reagents were from Sigma Chimie (La Verpillière, France).

Cell culture. Human promonocytic U-937 cells provided by Dr. Milon (Pasteur Institute, Paris, France) were *Mycoplasma*-free (tested at the *Mycoplasma* Unit of the Pasteur Institute, Paris, France) and were grown as reported elsewhere (20). This cell line lacks spontaneous adhesion, and all experiments were thus carried out on cells differentiated in the presence of 1,25-$(OH)_2$-cholecalciferol for 3–5 days (20).

Cell adhesiveness assay. Adhesiveness was measured in cells loaded with [*methyl*-^{3}H]thymidine as reported (22).

Measurement of $[Ca^{2+}]_i$. The cells were washed twice with buffer consisting of 125 mM NaCl, 5 mM KCl, 1 mM $MgCl_2$, 1 mM $CaCl_2$, 25 mM HEPES, pH 7.4, 5 mM glucose, and 2 mg/ml bovine serum albumin (2) and were resuspended in the same buffer supplemented with 2.5 mM probenecid to prevent fura-2 leakage. This buffer was used for all Ca^{2+} measurements, except for "Ca^{2+}-free" and "Mg^{2+}-free" conditions, in which these ions were omitted, and "Na^+-free" conditions, in which Na^+ ions were isosmotically replaced by choline.

Cell suspensions (2×10^6 cells/ml) were incubated with 1 μM fura-2/acetoxymethyl ester (as Ca^{2+} probe) for 45 min at 37° in the dark, washed, kept at room temperature (0.8×10^6 cells/ml), and used in <3 hr. The spectrofluorometer (SPEX F-112) was set at fixed wavelengths of 340 nm (excitation) and 510 nm (emission), except in Mn^{2+}-quenching experiments, which were carried out at the isosbestic point of the Ca^{2+}/fura-2 complex (360 nm). The calibration procedure was as follows: first, 6.6 mM EGTA/40 mM Tris was added to correct for extracellular fura-2 leakage and then F_{min} was estimated with 20 μg/ml digitonin and F_{max} with 10 mM $CaCl_2$.

Measurement of $[Ca^{2+}]_i$ in individual cells by scanning cytofluorometry. The cells were washed with the aforementioned buffer and then allowed to adhere to culture dishes (Nunc) for 1 hr at 37°, in buffer containing 1 mM fluo-3 as Ca^{2+} probe. After two washes, the cells were transferred to the dish holder of an ACAS 570 Meridian scanning cytofluorometer (23) and a group of cells was selected on the screen displaying the inverted microscope image. A 100- × 100-mm area including five to 10 cells was scanned at 10-sec intervals for 10–20 min. At the end of the scanning period, integration areas were drawn around each cell. The fluorescence of each area was calculated and converted into $[Ca^{2+}]_i$ by means of a calibration curve constructed with $[Ca^{2+}]_i$ standards, and individual time courses were plotted.

Measurement of intracellular IP_3 levels. The cells were washed and resuspended in RPMI 1640 medium supplemented with 2 g/liter bovine serum albumin and 25 mM HEPES, pH 7.4. Aliquots of the cell suspension, containing 10^7 cells in 500 μl, were prewarmed for 5 min at 37° and 100 μM La^{3+} was added if required, followed 1 min later by the agonists ADP or ATP. The incubation was stopped at various times from 10 to 30 sec, by addition of 125 μl of 20% perchloric acid. After vigorous vortex-mixing and centrifugation at 2000 × *g* for 20 min at 4°, the supernatants were neutralized with 1.5 M KOH/60 mM HEPES and the pH of each sample was checked with a microelectrode. The IP_3 content of the samples was quantified with a mass measurement technique, which employs the adrenal IP_3 receptor as binding protein.

Statistical analysis. The statistical analyses included (a) basic calculations (mean and standard error), (b) ANOVA model I, and (c) *a posteriori* comparisons using the Fisher LSD test between means for $\alpha = 0.05$ (24). Calculations were carried out using the Statview 512+ program on a Macintosh SE/30 microcomputer. EC_{50} values were calculated graphically. The traces shown are representative of at least three independent experiments with different cell preparations.

Results

Effects of P_2 purinergic agonists on cell adhesiveness. When differentiated U-937 cells were allowed to adhere to a plastic support, the percentage of adherent cells was maximal at 12 min and stabilized by 20 min. The percentage of adherent cells increased in the presence of 100 μM ADP or ATP (Fig. 1a). Surprisingly, the effect of ADP was greater than that of ATP. Concentration-response curves obtained at 12 min, the time of maximal effect, were bell-shaped; ATP and ADP became less efficient at the highest concentrations (Fig. 1b). This was not due to [*methyl*-^{3}H]thymidine leakage, thus excluding the presence of a permeabilizing P_{2z} receptor. The time course of the response to maximally effective concentrations (3 μM ATP and 50 μM ADP) (data not shown) was identical to that shown in Fig. 1a. This confirmed the greater efficacy of ADP over ATP. On the other hand, ATP was more potent than ADP, because the EC_{50} values, calculated on the ascending phase of the concentration-response curves, were 0.8 ± 0.17 and 13 ± 1.1 μM, respectively. The effects of several ATP and ADP agonists were tested to characterize the type of purinergic receptor involved in the adhesion response. UTP, UDP, and ATPγS concentration-response curves were also biphasic. The other analogues did not reach maximal effects. The rank order of potency based on the ascending phase of concentration-response curves was as follows: ATP = UTP > ATPγS > ADP = UDP > IDP = 2A5P > GDP > 2-Me-S-ATP > ADPβS. AMP-PCP, CDP, and 2-Me-S-ADP were completely ineffective. This ranking is in good agreement with that proposed for P_2 receptors of the nucleotide subtype, with which UTP and ATP are equipotent (9), whereas 2-Me-S-ATP, the head of the P_{2Y} series, is much less potent. 2-Me-S-ADP is the head of the P_{2T} series, and AMP-PCP is equipotent with ATP at P_{2z} receptors (5, 25).

The efficacy of ATP analogues did not match their potency (Table 1). ADP and, to a lesser extent, UDP were more effective but less potent than ATP, UTP, and ATPγS in promoting cell adhesion. PAF, an activator of phospholipase C, was as effective as ATP (Fig. 1c), but unlike ATP its concentration-response curve was monophasic, as shown previously (20). Extracellular Ca^{2+} is essential for the adhesion process. For instance, the Ca^{2+} chelator EGTA completely blocked adhesion (Fig. 1c). For this reason, we used Ca^{2+} channel blockers to test the role of

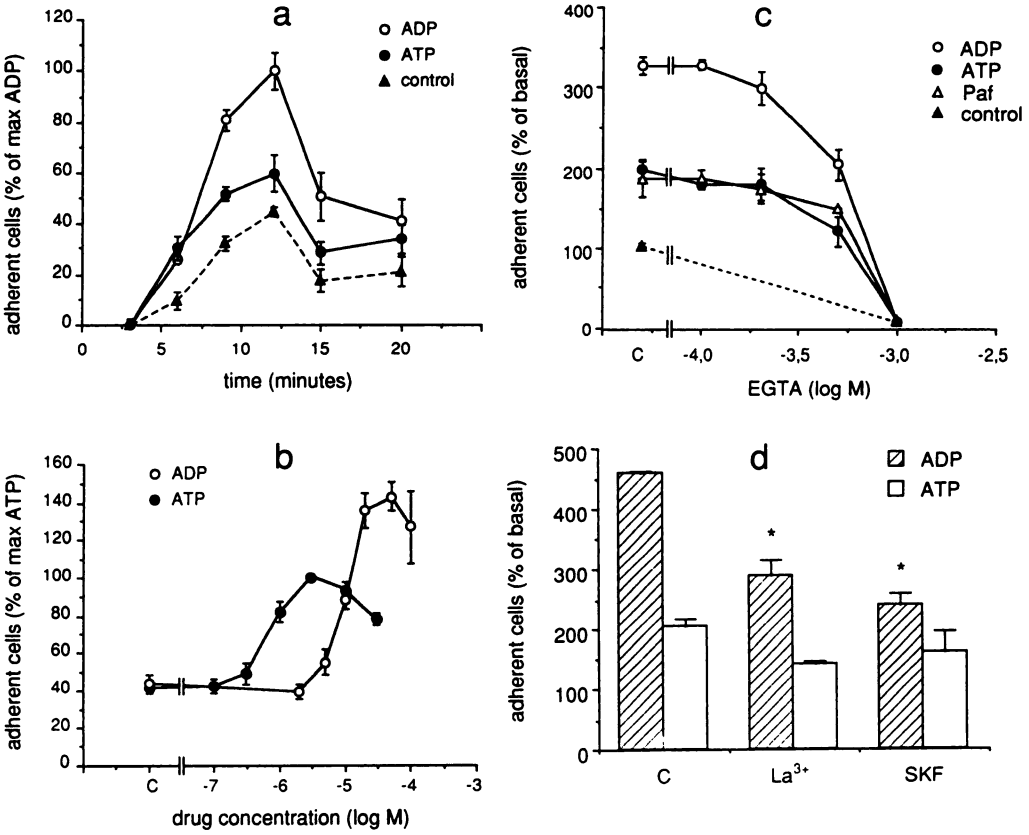

Fig. 1. Effects of ADP and ATP on cell adhesiveness. U-937 cells loaded overnight with [*methyl*-^{3}H] thymidine in Teflon flasks and resuspended in RPMI 1640 medium supplemented with 10% fetal calf serum and 25 mM HEPES were allowed to adhere to Petri dishes at 37° for various times, either spontaneously or in the presence of 0.1 mM ATP or ADP (a), for 12 min in the presence of increasing concentrations of ATP or ADP (b), for 12 min in the presence of increasing concentrations of EGTA, plus 0.1 μM PAF or 0.1 mM ATP or ADP as indicated (c), or for 12 min in the presence of 0.1 mM ATP or ADP, 0.1 mM La^{3+}, and 30 μM SKF-96365 (*SKF*) as indicated (d). The Ca^{2+} concentration in RPMI 1640 medium is 0.4 mM. The supernatants were discarded and adherent radioactive cells were recovered with 0.1% sodium dodecyl sulfate and counted by liquid scintillation counting. The results (mean ± standard error of triplicates) are representative of five (a), six (b), or two (c and d) experiments. *, Means significantly different from their controls (*C*) according to the LSD test (see Materials and Methods for details).

TABLE 1

Efficacy of ATP analogues in promoting cell adhesion

Maximally effective concentrations are reported; above these concentrations, the efficacy of ADP, UDP, UTP, and ATPγS decreased. Every concentration-response experiment included two controls, for spontaneous adhesion (*sa*) and 3 μM ATP-induced adhesion (*max*). The effect of each drug (*d*) is reported as a percentage of the effect of ATP, 100 × (*d* − *sa*)/(*max* − *sa*). Means ± standard errors are shown; *n* is the number of independent experiments, in triplicate.

Drug	Concentration	Effect*	*n*
	μM	% of ATP maximum	
ADP	50	176 ± 11.4	6
UDP	30	132 ± 11.1	5
UTP	10	94 ± 8.4	4
ATPγS	10	93	1
ADPβS	30	68 ± 5.0	2
2A5P	200	64 ± 17.5	2
2-Me-S-ATP	300	56 ± 4.5	2
IDP	300	47 ± 11.5	2
GDP	300	29 ± 2.0	2
CDP	300	13 ± 5.5	2
AMP-PCP	100	4 ± 1.0	2
2-Me-S-ADP	100	3 ± 0.5	2

* One-way ANOVA, $p < 0.0001$; Fisher LSD test, ADP ≠ UDP ≠ UTP = ATPγS ≠ ADPβS = 2A5P = 2-Me-S-ATP = IDP ≠ GDP ≠ CDP = AMP-PCP = 2-Me-S-ADP.

Ca^{2+} influx in the adhesive responses to ADP and ATP. La^{3+} (0.1 mM) and 30 μM SKF-96365 significantly inhibited the adhesive response to ADP but not to ATP (Fig. 1d). These results suggested that different mechanisms might be involved in the responses to ADP and ATP and prompted us to investigate the signaling pathways of these nucleotides.

Effects of ADP and ATP on $[Ca^{2+}]_i$ and intracellular IP_3 levels. Both ADP and ATP increased $[Ca^{2+}]_i$. The time course of the responses was drug and concentration dependent (Fig. 2). In the case of ADP, the slopes of both the rise and the fall of the response sharpened as drug concentrations increased (Fig. 2, *upper*). Sustained plateau levels were obtained at up to 10 μM, and above this concentration a slow return to base-line was observed. In contrast, ATP evoked an initial spike, the height and amplitude of which increased in a concentration-dependent manner up to 1 μM (Fig. 2, *lower*). Above 10 μM, the duration of the spike was reduced by a sharp fall to base-line, but a second rise in $[Ca^{2+}]_i$ to moderate but sustained levels occurred. When the time scale was expanded, a lag of 5–6 sec was observed for ADP but not for ATP (Fig. 3), even at concentrations as low as 0.1 μM.

IP_3 levels were measured between 10 and 30 sec after addition of the nucleotides (Fig. 3). Two ranges of concentrations were chosen. High (10 μM) ADP and ATP concentrations were maximally effective on $[Ca^{2+}]_i$. In this case, the time course of IP_3 levels matched the $[Ca^{2+}]_i$ rise; the response of both parameters to ATP was rapid and strong, whereas the response to ADP was weaker and developed slowly throughout the 30-sec study period. Low (5 μM ADP and 100 nM ATP) concentrations evoked "pure" plateau or spike $[Ca^{2+}]_i$ responses, respectively. In this case, the small increases in IP_3 levels observed were not statistically significant.

The effects of various ATP and ADP analogues on $[Ca^{2+}]_i$ were tested to obtain their rank order of potency. Two groups of drugs were identified according to the time course of the response (Fig. 4). ADPβS, like ADP, evoked a plateau, whereas UTP, ATPγS, UDP, IDP, 2A5P, GDP, and 2-Me-S-ATP mimicked the effect of ATP with a spike, sometimes followed by a plateau. As observed in adhesion studies, 2-Me-S-ADP, CDP, and AMP-PCP were ineffective. Concentration-response

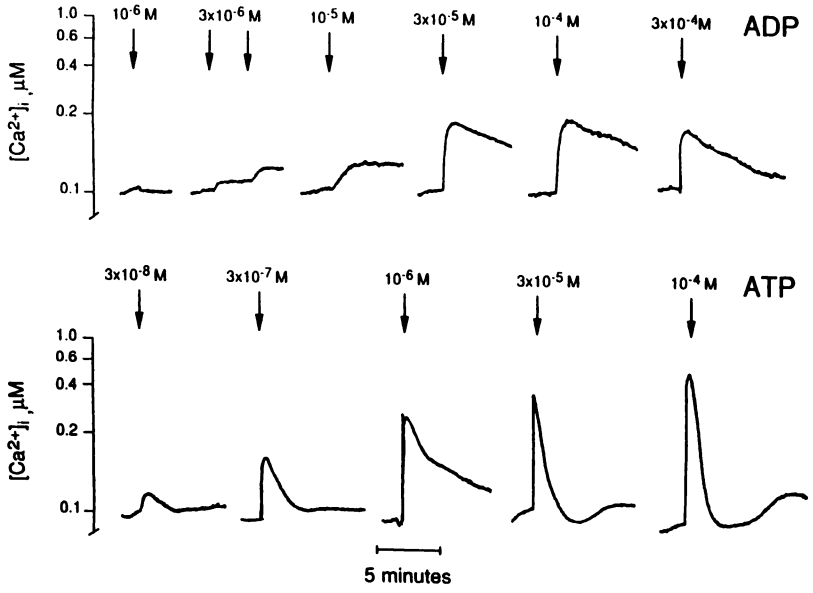

Fig. 2. Effects of ADP and ATP on $[Ca^{2+}]_i$ measured in cell populations. The time courses of the fluorescence changes induced by various concentrations of ADP and ATP in separate batches of fura-2-loaded cells are shown. The time constant was 1 sec (see Materials and Methods for details).

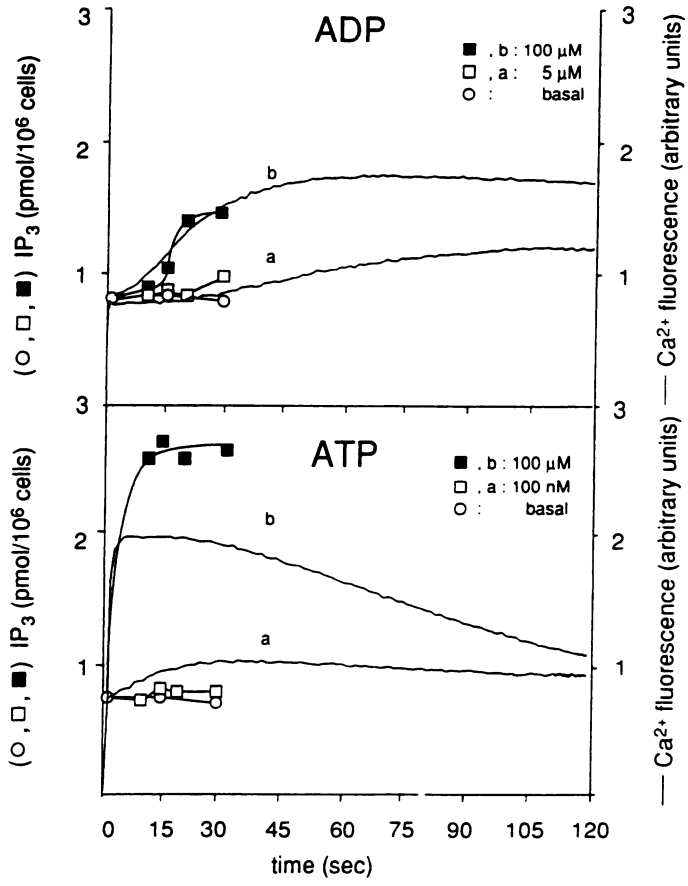

Fig. 3. Short term effects of ADP and ATP on IP_3 levels and $[Ca^{2+}]_i$. The effects of ADP and ATP on IP_3 (*symbols*) and $[Ca^{2+}]_i$ (*traces*) are plotted in an expanded time scale of 120 sec. IP_3 was determined by a mass measurement technique and $[Ca^{2+}]_i$ by fura-2 fluorescence of cell populations, with a time constant of 1 sec (see Materials and Methods). Low (5 μM ADP or 100 nM ATP) and high (100 μM) concentrations of nucleotides were tested. IP_3 levels (means of three experiments in duplicate) and representative Ca^{2+} fluorescence traces are shown. The effect of high but not low concentrations of nucleotides on IP_3 levels was significantly different from base-line (ANOVA and Fisher LSD test).

curves were drawn from maximal $[Ca^{2+}]_i$ evoked by each drug concentration. The rank order of potency of the analogues was similar to that obtained in adhesion experiments. Maximal $[Ca^{2+}]_i$ values were induced by 100 μM ATP (478 ± 32 nM versus 91 ± 3.4 nM basal level), UTP, UDP, and ATPγS (100 ± 0.8%, 97 ± 1%, and 88 ± 5% of the ATP response, respectively). ADP was less efficient (54 ± 6%) and also less potent than ATP. The EC_{50} values (16 ± 2.8 μM for ADP and 0.5 ± 0.14 μM for ATP) were of the same order of magnitude as those obtained in cell adhesion experiments.

The efficacy and potency of ADP and ATP were similar in the presence and absence of Mg^{2+} ions. This indicates that the free acid species of the nucleotides is not the active form, ruling out the presence of a P_{2x} receptor (3).

Individual cell responses to ADP and ATP were studied by scanning cytofluorometry. Spontaneous $[Ca^{2+}]_i$ oscillations of low amplitude and a 20–30-sec period were observed in all of the cells studied (data not shown). The effect of low concentrations of agonist, able to evoke pure plateau or spike responses and also used in the experiments of Fig. 3, was tested. Distinct cellular responses to 0.1 μM ATP (86 cells) or 5 μM ADP (85 cells) were observed, even in the same batch of cells. The responses were sorted on the basis of their temporal pattern, as shown in Fig. 5. Type 1 is a spike, type 2 a sharp rise followed by a slow return to base-line, and type 3 a peak followed by a secondary wave. In contrast, types 4 and 5 correspond to slow and moderate rises in $[Ca^{2+}]_i$, either transient (type 4) or persistent (type 5). The slow return to basal levels, the secondary wave, and the slow response often consisted of a train of oscillations with a period of about 20 sec (data not shown). The frequency distribution of the different response patterns is shown in Fig. 5. The majority of the responses to ATP were type 1 and type 2, that is, rapid and short (92%), whereas the responses to ADP lasted longer (no type 1, types 2 + 3 = 58%), were delayed (types 4 + 5 = 23%), or null (19%). Thus, in spite of some overlap, the patterns of response to low concentrations of ADP and ATP were clearly different.

The coexistence of independent ADP and ATP receptors was further investigated by sucessive additions of both nucleotides to the same cells. Above 10 μM, ATP pretreatment completely

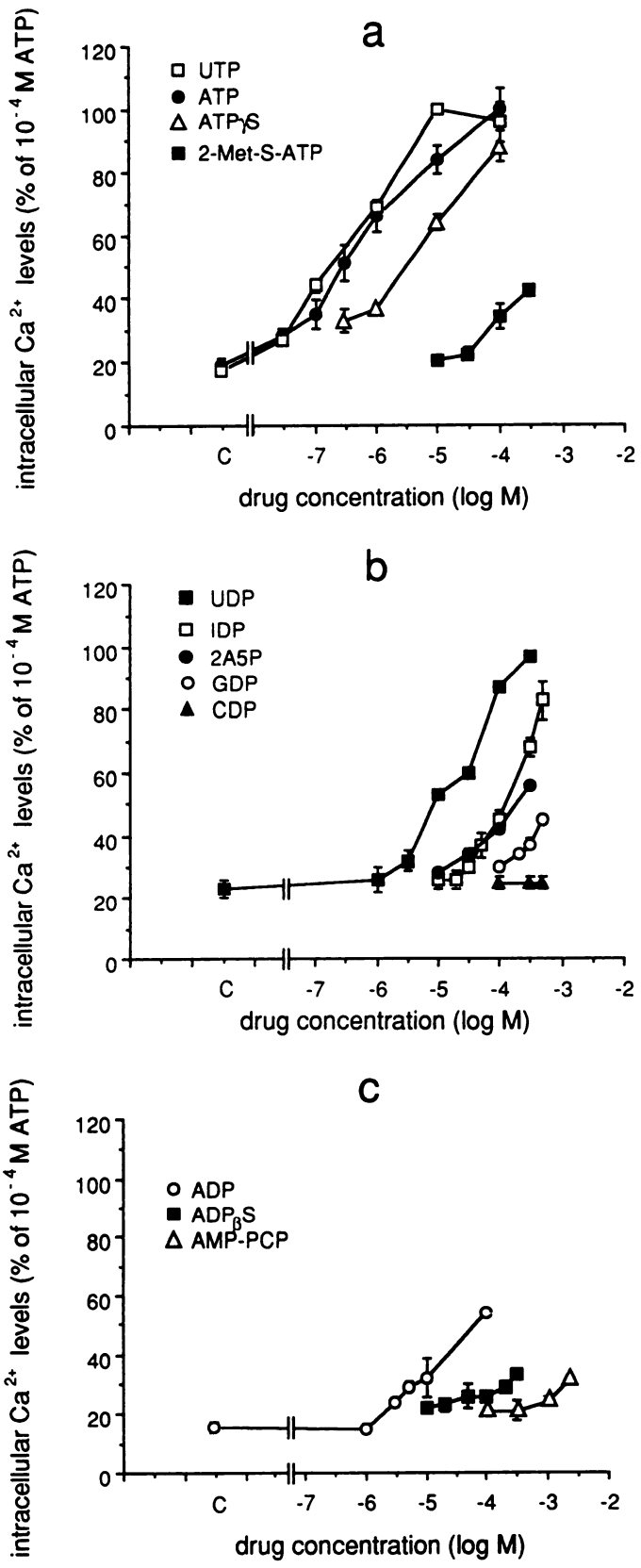

Fig. 4. Concentration-dependent effects of ATP analogues on $[Ca^{2+}]_i$ measured in cell populations. The effects of ATP analogues on $[Ca^{2+}]_i$ was determined by fura-2 fluorescence (see Materials and Methods). a and b, The analogues displayed a time course similar to that of ATP, i.e., basically a spike. c, The analogues displayed a time course similar to that of ADP, i.e., a plateau. Each experiment included all points of a concentration-response curve obtained on the same day on the same cell preparation, including an ATP control. Means of two to four experiments are shown.

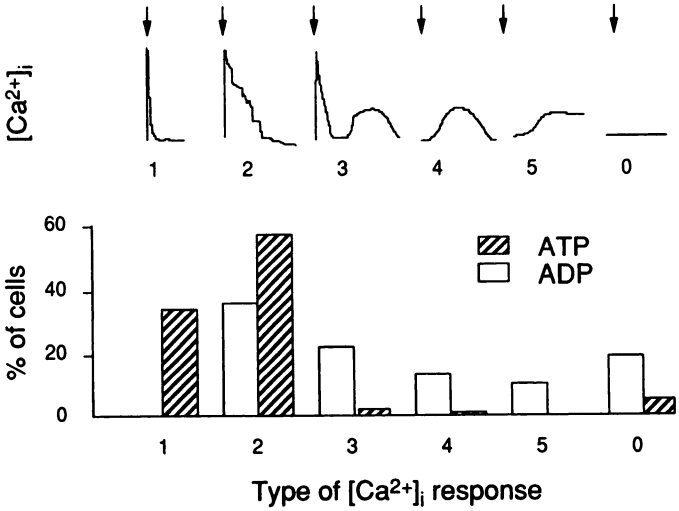

Fig. 5. Frequency distribution of the effects of ADP and ATP on the $[Ca^{2+}]_i$ measured in individual cells. Fluo-3 fluorescence changes induced by low nucleotide concentrations, as a function of time, were studied in individual cells by scanning cytofluorometry (see Materials and Methods). $[Ca^{2+}]_i$ responses to 5 μM ADP and 0.1 μM ATP were sorted according to the time course patterns shown (*1-0*) (*upper*). *Arrows*, time when the nucleotide was added. The number of cells displaying a given response were plotted as a percentage of the total number of cells (85 for ADP and 86 for ATP) scanned on different days (*lower*).

abolished the response to ATP itself but also that to ADP (Fig. 6). On the other hand, as shown in Fig. 2, the effect of low (3 μM) ADP concentrations was additive. Concentrations of ADP higher than 10 μM were still effective, although they did not produce further increments in $[Ca^{2+}]_i$. ATP addition at this point still evoked a peak, followed by a sharp fall to pre-ADP levels (data not shown). The peak and the return to basal levels evoked by ATP in ADP-pretreated cells are shown in Fig. 6. Thus, ADP decreased but did not block the response to ATP. Several mechanisms are potentially involved in these effects, i.e., competition at the receptor level, desensitization, and depletion of Ca^{2+} stores. The first two of these three mechanisms were investigated in cells adherent to a quartz slide, to allow washing of the cuvette contents. Homologous desensitization was observed for 10 μM ATP and ADP; after washing, the responses to these nucleotides were reduced to 43 ± 6% and 35 ± 3%, respectively. With respect to cross-desensitization, after 100 μM ATP pretreatment and washing 31 ± 2% of the response to 100 μM ADP was recovered. Conversely, pretreatment with 100 μM ADP followed by washing did not modify the response to 0.3 μM ATP. Depletion of Ca^{2+} stores did not play a role in these phenomena, because pretreatment of the cells with the phospholipase C activator PAF only partly decreased the response to both ATP and ADP, and vice versa (Fig. 6). These results also show that heterologous desensitization between purinergic and nonpurinergic agonists is irrelevant in U-937 cells. As already mentioned, in ADP-treated cells the slow return to basal levels was accelerated by ATP. Interestingly, PAF was ineffective in this regard (Fig. 6). Taken together,

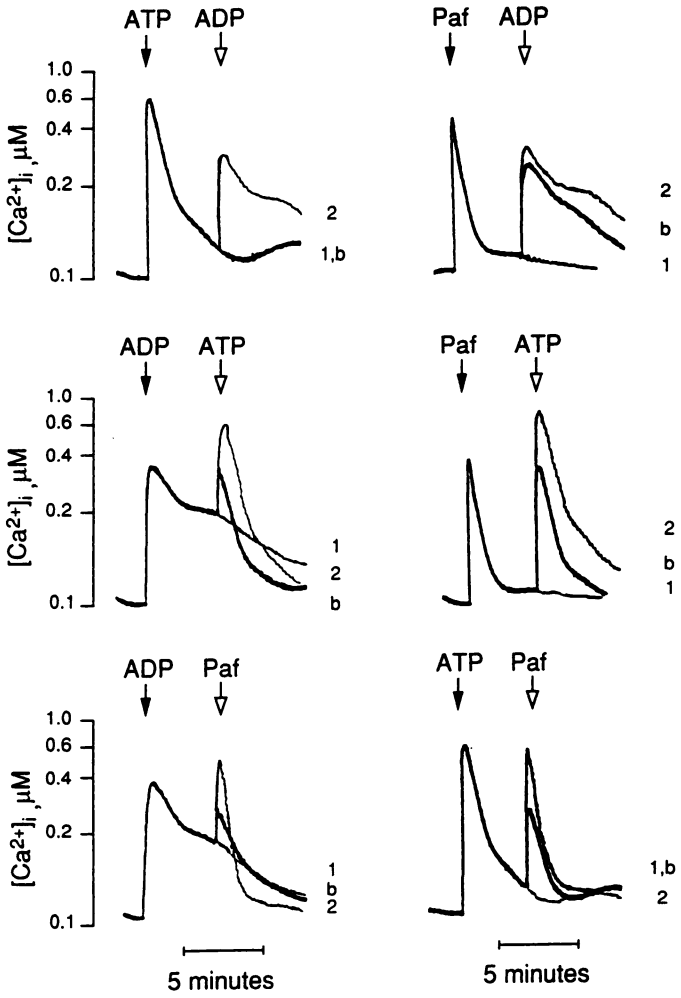

Fig. 6. Effects of pretreatment with ADP, ATP, or PAF on subsequent Ca^{2+} responses to these agonists. The time courses of the fluorescence changes induced by 10 μM ADP, 10 μM ATP, or 0.1 μM PAF in fura-2-loaded cells pretreated with these agonists (*arrows*) are shown. *After the black arrows*, every *trace* shows the effect of the indicated agonist. *After the white arrows*, three *traces* are shown; *1* (first), end of the trace with the first agonist alone; *b* (both) (the largest), effect of addition of the second agonist; *2* (second), effect of the second agonist alone, superimposed for comparison.

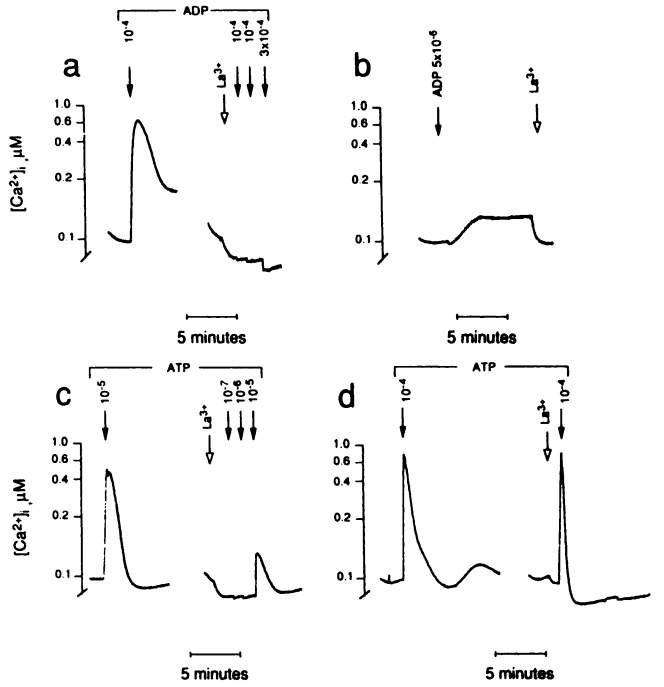

Fig. 7. Effects of La^{3+}, a Ca^{2+} channel blocker, on the Ca^{2+} response of cell populations to ADP and ATP. The time courses of the fluorescence changes induced by various concentrations of ADP (a and b) and ATP (c and d) in different batches of fura-2-loaded cells in the absence or presence of 100 μM $LaCl_3$ are shown. ADP, ATP, and La^{3+} were added at the times indicated (*arrows*).

these results suggest that ATP blocks the response to ADP at the receptor level, whereas the reverse is not true.

Dependence of the $[Ca^{2+}]_i$ rise on extracellular Ca^{2+}. To assess the dependence of the $[Ca^{2+}]_i$ rise on extracellular Ca^{2+}, the responses to ADP and ATP were studied in the presence of 100 μM La^{3+}, a Ca^{2+} channel blocker. The response to ADP was inhibited under these conditions (Fig. 7a). Moreover, plateau $[Ca^{2+}]_i$ evoked by ADP rapidly fell to base-line upon addition of La^{3+} (Fig. 7b). For ATP, in the presence of La^{3+} the concentration-response curve of the spike response was shifted to the right (EC_{50} of 15 ± 1.0 μM versus 0.46 ± 0.14 μM in the presence of Ca^{2+}), but maximal efficacy was obtained (Fig. 7c). In contrast, the plateau component of the response was abolished (Fig. 7d). In nominally Ca^{2+}-free medium and in the presence of 6.6 mM EGTA, the responses to ADP and ATP were as described for La^{3+}. Thus, it appears that the $[Ca^{2+}]_i$ rise induced by ADP relied on Ca^{2+} influx, whereas ATP activated both Ca^{2+} mobilization and Ca^{2+} influx.

The "Ca^{2+} reintroduction" protocol, that is, the addition of Ca^{2+} to cells with empty Ca^{2+} stores, was designed to study receptor-activated Ca^{2+} influx. However, it soon appeared that depletion of Ca^{2+} stores itself evoked Ca^{2+} entry. Fig. 8 shows the effect of 1 mM Ca^{2+} addition to cells kept in nominally Ca^{2+}-free medium. ADP had no effect when added either before (Fig. 8a) or at the height of (Fig. 8b) the response. Thus, in U-937 cells, ADP-induced and "store-operated" Ca^{2+} influxes are not additive. Conversely, a small decrease in $[Ca^{2+}]_i$ was evoked by ATP (data not shown). This is reminiscent of the inhibitory effect of ATP on ADP-pretreated cells, in which the return to basal levels was accelerated by ATP (Fig. 6). Ca^{2+} influx can also be assessed as Mn^{2+} entry-induced quenching of the fluorescence signal at the isosbestic point for Ca^{2+} (360 nm). Fig. 8c shows that the slope of Mn^{2+} entry was steeper in the absence than in the presence of extracellular Ca^{2+}. This confirms the presence of store-operated Ca^{2+} influx in U-937 cells. Accordingly, Mn^{2+} entry was activated by ADP (Fig. 8c) and ATP (data not shown) in the presence but not in the absence of extracellular Ca^{2+}.

Subsequent experiments were carried out in the presence of 1 mM Ca^{2+} and 100 mM Mn^{2+} to avoid store-operated Ca^{2+} influx but also because the slope of basal Mn^{2+} influx was steep even in the presence of Ca^{2+}. This pointed either to spontaneous or background (26) Ca^{2+} influx through "leaky" channels or to some degree of cell activation under our experimental conditions. The time courses of ADP- and ATP-evoked Ca^{2+} influx were again different. The effects of ADP were slow and long-lasting, and the slope was concentration dependent. In contrast, ATP induced a rapid decrease in fluorescence. Mn^{2+} entry, either basal or activated by ADP or ATP, was blocked by equimolar concentrations of La^{3+} (data not shown).

The effect of 100 μM La^{3+} on IP_3 levels evoked by ADP and

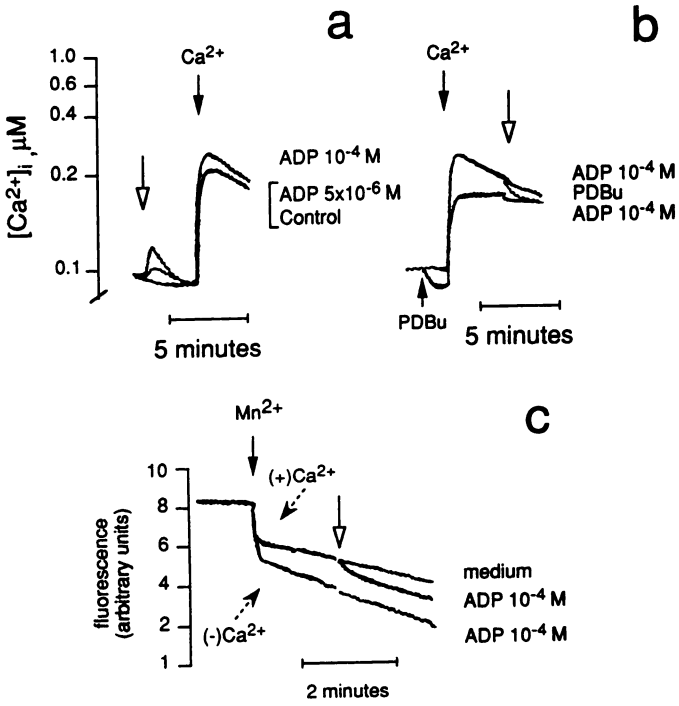

Fig. 8. Effects of ADP on store-operated Ca^{2+} influx. a and b, Time courses of the fluorescence changes induced by 1 mM $CaCl_2$ in fura-2-loaded cells kept in Ca^{2+}-free medium. Excitation wavelength, 340 nm. a, Cells were pretreated with medium (*Control*) or ADP (*white arrow*). b, ADP (*upper trace, open arrow*), PDBu (*middle trace, open arrow*), or both (*lower trace*, PDBu, *filled arrow*; ADP, *open arrow*) were added as indicated. c, Time courses of the fluorescence changes induced by 100 μM $MnCl_2$ and ADP in fura-2-loaded cells kept in 1 mM $CaCl_2$-containing medium or in Ca^{2+}-free medium, as indicated (*arrows*). The excitation wavelength was 360 nm, the isosbestic point for the fura-2/Ca^{2+} complex.

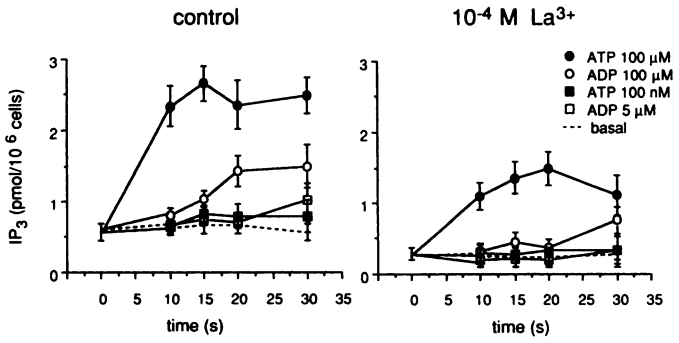

Fig. 9. Effects of La^{3+} on the IP_3 response to ADP and ATP. U-937 cells were incubated with ADP or ATP at the indicated concentrations for various times, in the absence or presence of 100 μM $LaCl_3$, a Ca^{2+} channel blocker. IP_3 content (pmol/10^6 cells, mean ± standard error of four experiments) was determined by a mass measurement method (see Materials and Methods). In a three-way ANOVA the nucleotide and $LaCl_3$ factors were highly significant ($p < 0.001$), whereas the time factor was not significant.

ATP is shown in Fig. 9. La^{3+} completely inhibited the response to ADP, even at 10 μM, whereas the response to 10 μM ATP was reduced by 40%. Thus, it appears that Ca^{2+} influx was required for ADP to evoke an increase in IP_3 levels. Conversely, Ca^{2+} influx contributed to, but was not essential for, the IP_3 response to ATP.

To determine the role of the Na^+/Ca^{2+}-exchanger in Ca^{2+} movements, NaCl was isosmotically replaced by choline in the medium in some experiments. This did not modify the Ca^{2+} responses to ADP or ATP (data not shown).

Role of G proteins and protein kinases in ADP- and ATP-induced $[Ca^{2+}]_i$ responses. We investigated the participation of G proteins in the responses to ADP and ATP, by pretreatment of cells with pertussis toxin (120 ng/ml, for 24 hr) or cholera toxin (0.5 μg/ml, for 3 hr). Neither the time courses nor the concentration-response curves were modified (data not shown). Thus, the ADP and/or ATP receptors of U-937 cells are not coupled to pertussis or cholera toxin-sensitive G proteins.

Pretreatment with the protein kinase C activator PDBu (160 nM, for 2 min) before addition of ATP shifted the concentration-response curve of spike $[Ca^{2+}]_i$ to the right (EC_{50} = 15 ± 1.4 μM), accelerated the return to base-line, and prevented the plateau phase (Fig. 10, a and b). In the case of ADP, PDBu pretreatment completely inhibited the response to 100 μM ADP (Fig. 10d). Moreover, when added after ADP, PDBu returned $[Ca^{2+}]_i$ to pre-ADP levels in <30 sec (Fig. 10c). All of these

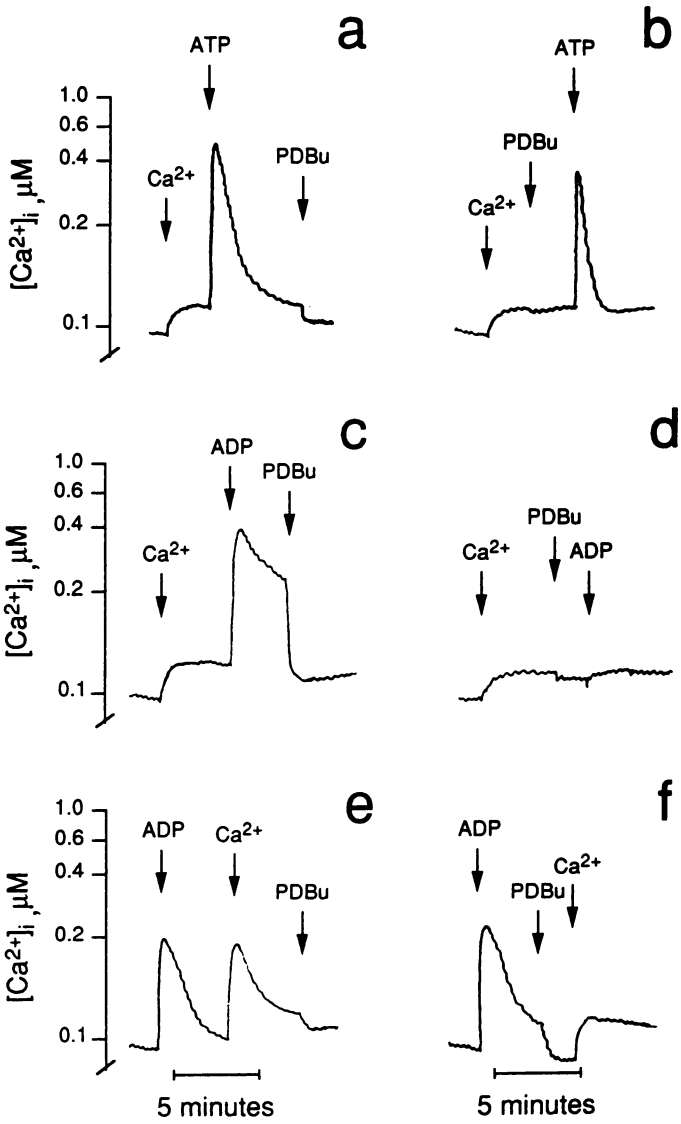

Fig. 10. Effects of PDBu on the Ca^{2+} response to ADP and ATP. The time courses of the fluorescence changes induced in fura-2-loaded cells by 160 nM PDBu and 1 mM $CaCl_2$, added before or after 100 μM ADP or ATP as indicated (*arrows*), are shown.

effects are reminiscent of those observed in the presence of the Ca^{2+} channel blocker La^{3+}. In these experiments, carried out in normal (1 mM Ca^{2+}-containing) medium, 1 mM Ca^{2+} was further added to show that background Ca^{2+} influx, probably through leaky channels, was not modified by PDBu, whereas ADP-evoked Ca^{2+} influx was indeed blocked (see also Fig. 10, e and f). An interesting finding was that, as shown in Fig. 8b, PDBu did not block store-operated Ca^{2+} influx. The indirect study of Ca^{2+} influx by Mn^{2+} quenching showed that 160 nM PDBu had no effect by itself but completely blocked the effect of ADP (Fig. 11b). In contrast, the rapid influx component of the response to ATP was still present (Fig. 11a). Preliminary data indicated that this rapid component was in turn inhibited in a concentration-dependent manner by the kinase inhibitor wortmannin, whereas wortmannin was less potent in inhibiting ADP- than ATP-induced Ca^{2+} influx. Moreover, the effects of wortmannin and PDBu on ATP-evoked Ca^{2+} influx were additive (data not shown). As shown in Fig. 11c, working conditions were isosbestic in Mn^{2+}-quenching experiments.

To test the role of the cAMP/protein kinase A pathway, cells were treated with drugs known to increase cAMP levels. Neither the efficacy nor the potency of ADP or ATP was modified by previous (2–5 min) or simultaneous treatment with 1 μM PGE_1 or 10 μM isoproterenol or pretreatment with 1 mM 8-bromo-cAMP for 15 min. Fig. 12b illustrates the absence of effect of PGE_1 on the spike response evoked by ATP. However, a time-dependent effect was observed on plateau $[Ca^{2+}]_i$ after addition of PGE_1, isoproterenol, or the P_1 agonist 2-chloroadenosine. As shown in Fig. 12a, when PGE_1 was added simultaneously with 5 μM ADP or in the ascending phase of the plateau response, the elevation of $[Ca^{2+}]_i$ was delayed but reached the same range as in controls. In cells exhibiting plateau $[Ca^{2+}]_i$, PGE_1 treatment resulted in a transient fall in $[Ca^{2+}]_i$, lasting <5 min. This fall was observed whatever the origin of the plateau response, i.e., either low ADP concentrations or the secondary Ca^{2+} wave evoked by ATP (Fig. 12, a and c). The effects of PGE_1 and isoproterenol were further characterized in cells treated with 5 μM ADP to obtain plateau $[Ca^{2+}]_i$. Alprenolol, a β-adrenergic antagonist, inhibited the effect of isoproterenol but not that of PGE_1. The IC_{50} was 4.5 ± 2.5 nM for isoproterenol and 48 ± 9.8 nM for PGE_1. The latter was shifted to 9.5 ± 0.78 nM by pretreatment for 15 min with 100 μM Ro-20,174, a cAMP-phosphodiesterase inhibitor (data not shown). The inhibitory effect of PGE_1 was partly blocked in cholera toxin- or 8-bromo-cAMP-treated cells, likely due to receptor desensitization, and was slightly potentiated in pertussis toxin-treated cells. These data strongly suggest that cAMP was involved in the inhibitory effects of PGE_1 on $[Ca^{2+}]_i$. On the other hand, PGE_1 was completely ineffective in Mn^{2+}-quenching studies. This indicates that Ca^{2+} influx competed with by Mn^{2+} was not the primary target of PGE_1.

Discussion

The aim of this work was to correlate the effects of ADP and ATP on cell adhesion with their signaling pathway(s). U-937 cells acquire adhesive properties along differentiation towards a more monocytic phenotype. For this reason the studies presented here were carried out in promonocytic U-937 cells differentiated with 1,25-dihydroxy-vitamin D_3 (20). Incidentally, we found in preliminary experiments that the time courses of the $[Ca^{2+}]_i$ responses to ADP and ATP were similar in undif-

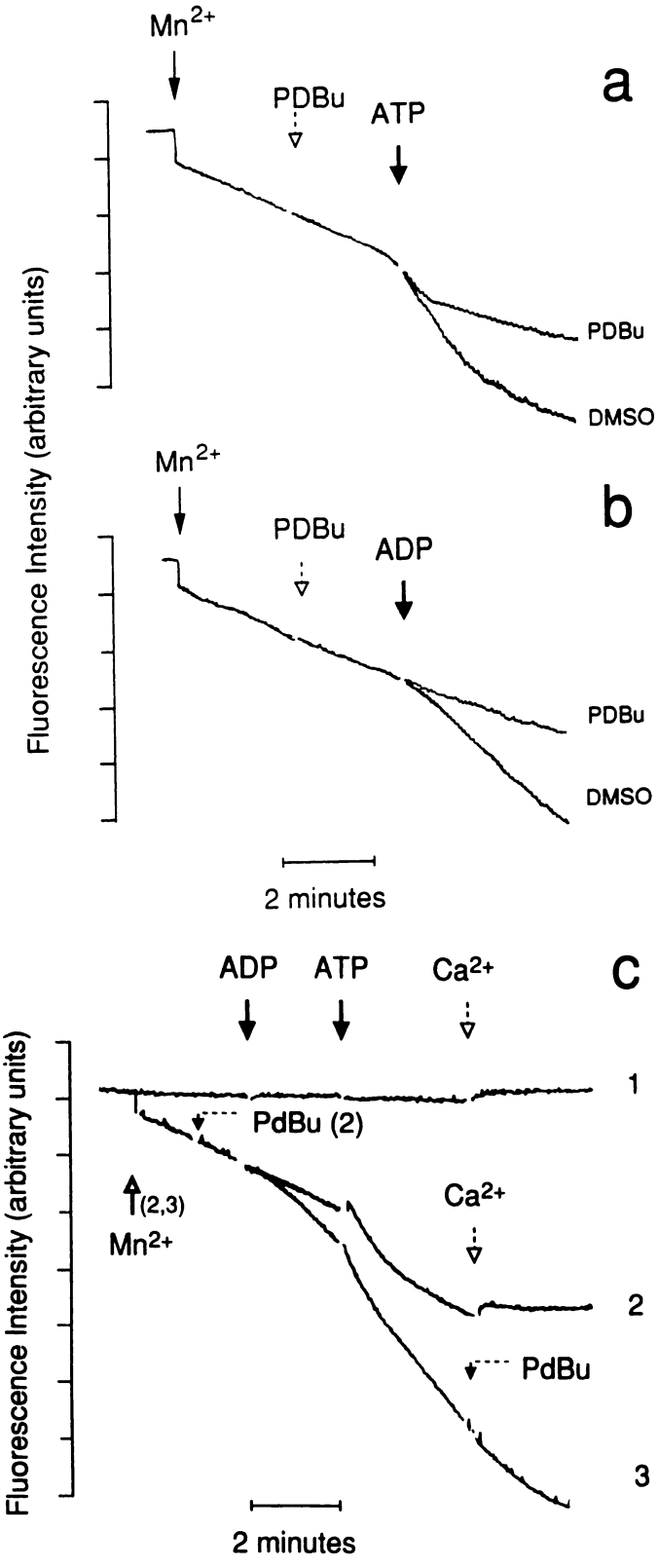

Fig. 11. Effects of PDBu on ADP- and ATP-evoked Ca^{2+} influx. Fluorescence traces as a function of time were recorded at 360-nm excitation wavelength, in the presence of the Ca^{2+} surrogate Mn^{2+}. a and b, Effects of addition of 100 μM ADP or ATP to cells pretreated with 160 nM PDBu or its solvent, dimethylsulfoxide (*DMSO*). c, Effects of subsequent additions of ADP and ATP in the presence or absence of PDBu (*traces 2* and *3*). Working conditions were isosbestic (*trace 1*).

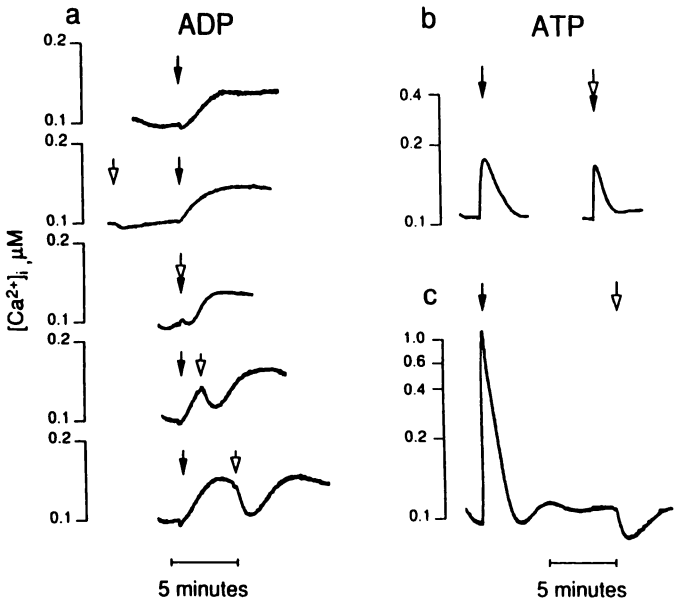

Fig. 12. Effects of PGE_1 on the Ca^{2+} response to ADP and ATP. The time courses are shown for the fluorescence changes induced in fura-2-loaded cells by 1 μM PGE_1 (*white arrows*) added before, together with, or after the nucleotides (*black arrows*) at the following concentrations: a, 5 μM ADP; b, 100 nM ATP; c, 100 μM ATP.

ferentiated and differentiated cells. These results are in agreement with the data of Cowen *et al.* (2) showing no evolution of the ATP responses in neutrophil/monocyte progenitors.

We have found that the $[Ca^{2+}]_i$ response to ADP, but not to ATP, is strictly dependent on Ca^{2+} influx. Moreover, ADP and ATP activate distinct Ca^{2+} influx mechanisms. These results suggest that ADP and ATP activate distinct signaling pathways in U-937 cells. ADP and ATP have been shown to behave differently in various cell systems. In platelets, ATP is a competitive antagonist of the effects of ADP (3). In aequorin-loaded hepatocytes, the existence of distinct receptors has been evoked to explain the different Ca^{2+} oscillation patterns induced by ADP and ATP (27). In endothelial cells, ADP has been reported to mobilize intracellular Ca^{2+} in an IP_3-independent manner, whereas ATP activates the phospholipase C signaling pathway (28).

The time courses of the $[Ca^{2+}]_i$ responses to ADP and ATP were different. The response to ATP was biphasic, with a $[Ca^{2+}]_i$ spike followed by a plateau, whereas the response to ADP was limited to the plateau. The study of individual $[Ca^{2+}]_i$ responses in cells transfected with distinct receptor isoforms has shown that the pattern of response depends on the molecular structure of the receptor. Activation of the muscarinic m2 variant evokes slow, oscillatory, and focal release mediated by a pertussis toxin-sensitive G protein, whereas the m3 variant induces a propagating, pertussis toxin-insensitive, Ca^{2+} wave (29). The m2 variant couples to $G_{\alpha i}$ and releases free $\beta\gamma$ subunits, which in turn activate phospholipase C-$\beta_{3/2}$, whereas the m3 variant directly activates phospholipase C-$\beta_{1/3}$ through $G_{\alpha q/11}$ (30, 31). The activation of vascular smooth muscle cells by different isoforms of PDGF also results in different patterns of $[Ca^{2+}]_i$; PDGF-AA causes oscillations dependent on extracellular Ca^{2+}, whereas PDGF-BB elicits a monophasic response (32). Indeed, PDGF A and B chains bind to distinct α or β isoforms of the dimeric receptor. PDGF activates phospholipase C-γ through the tyrosine kinase activity of PDGF receptors (31). Thus, it appears that each phospholipase C activation mechanism is able to generate distinct patterns of response, depending on the receptor isoform involved. Accordingly, we suggest that spike and plateau effects in U-937 cells may be mediated by distinct receptor molecules. An "ATP receptor" could primarily evoke the $[Ca^{2+}]_i$ spike, whereas an "ADP receptor" could mediate the slow, delayed, and Ca^{2+} influx-dependent plateau response. Above 10 μM, ATP could activate the ADP receptor as well. This dual-receptor hypothesis is further supported by the results of desensitization studies and by individual cell $[Ca^{2+}]_i$ responses to low concentrations of nucleotide. Interestingly, an ADP receptor with a sequence different from that of the chicken brain ATP receptor has been obtained from the same source (33). Indeed, the possibility that each agonist preferentially couples to separate pathways (distinct G proteins, phospholipase C isoforms, or other effectors) through the same receptor molecule cannot be excluded. Moreover, a recent report indicates that thrombin and agonist peptide, despite being agonists for a common receptor, induce dissimilar $[Ca^{2+}]_i$ responses (34). Composite responses are observed in both models. Similarly, the plateau is Ca^{2+} influx dependent and inhibitable by phorbol esters. However, the single component isolated differs, i.e., the spike in the case of thrombin and the plateau in the case of ADP. This means that, in contrast to the agonist peptide-induced plateau, the ADP-induced plateau is independent of the spike.

There is strong evidence that the $[Ca^{2+}]_i$ spike evoked by receptors coupled to phospholipase C is supported by IP_3 mobilization of intracellular stores (35). In our model, the spike evoked by ATP, which is clearly linked to Ca^{2+} mobilization, implies that the ATP receptor primarily couples to phospholipase C and secondarily activates Ca^{2+} influx. In the case of ADP, Ca^{2+} influx precedes and is required for the rise in $[Ca^{2+}]_i$, phospholipase C activation, and IP_3 production. The "spike" or ATP receptor of U-937 cells that couples to phospholipase C could be the P_{2U} subtype (9), because UTP was equipotent with ATP, whereas 2-Me-S-ATP, the head of the P_{2Y} series (3), and ADPβS, a good ligand for this receptor (36), were poor agonists. Its effect is probably mediated by phospholipase C-β_3 through $G_{\alpha 16}$, because these isoforms were detected in our U-937 cells by Western blotting.[1] $G_{\alpha i2}$, small amounts of $G_{\alpha q}$, and phospholipase C-γ_1 were also detected.

There are several explanations for the plateau $[Ca^{2+}]_i$ response also evoked by ATP. First, the effect of ATP could be due to its dephosphorylation product ADP, because ectophosphatase activity has been detected in several cell types (3). However, ADP formation is negligible under the experimental conditions used in Ca^{2+} studies.[2] More likely, ATP can bind to the ADP receptor as well, possibly with lower affinity, because the plateau appears at higher ATP concentrations.

The mechanisms involved in receptor-activated Ca^{2+} influx are still elusive (37). Ligand-gated, G protein-coupled, and second messenger-activated Ca^{2+} channels have been described (37). In U-937 cells, at least three Ca^{2+} influx mechanisms exist, as shown by Mn^{2+}-quenching studies, all of them inhibitable by La^{3+}; the first is background influx, also evidenced by means of increasing extracellular Ca^{2+} levels (26), which is insensitive to PDBu and wortmannin, the second is rapid

[1] Dr. M. Camps, German Cancer Research Center, Heidelberg, Germany, personal communication.
[2] M. A. Ventura, unpublished observations.

influx, which is evoked by ATP, is insensitive to PDBu, and probably is inhibited by wortmannin, and the third is slow influx, which is activated by ADP and high ATP levels, is less sensitive to wortmannin, and is inhibited by PDBu. Several Ca^{2+} entry pathways have been suggested in fibroblasts and Jurkat T cells (38). Similarly, in thrombin-activated platelets, 6 μM wortmannin, a kinase inhibitor, discriminated rapid (within 3 sec) and slow (within 3 min) Ca^{2+} influx studied with the Ca^{2+} reintroduction protocol in platelets (39). However, in this case the slow component was preferentially affected. Wortmannin inhibits myosin light chain kinase activity in the micromolar range and PI3K activity in the nanomolar range. The latter enzyme is activated by tyrosine phophorylation. Recently, an isoform of PI3K activated by ATP via the $\beta\gamma$ subunits of trimeric G proteins and inhibited by wortmannin in the low micromolar range was described in U-937 cells (40). Because ATP mobilizes intracellular Ca^{2+} stores, rapid Ca^{2+} influx induced by ATP probably corresponds to capacitative Ca^{2+} entry (37), which indeed exists in U-937 cells (Fig. 8). Based on the inhibition of rapid Ca^{2+} influx by wortmannin, we suggest a link between capacitative Ca^{2+} entry and PI3K activity. This hypothesis is currently under study.

With respect to slow Ca^{2+} influx, a lag of several seconds is hardly compatible with opening of a Ca^{2+} channel by the agonist. Direct activation of Ca^{2+} release-activated channels by an agonist receptor has been proposed (37). This could explain the fact that store-operated Ca^{2+} entry and ADP-induced Ca^{2+} entry are not additive. In this case, PDBu and wortmannin effects would take place upstream in the ADP and ATP signaling pathways, which would converge at the Ca^{2+} channel level. Influx could also be carried by a G protein-coupled or second messenger-activated Ca^{2+} channel (37). We found no depolarizing effect of ATP or ADP with the fluorescent probe bisoxonol in U-937 cells.[3] A nonselective, ATP-activated, G protein-dependent, Ca^{2+} conductance has been documented in HL-60 cells by patch-clamp studies (41). However, this effect was pertussis toxin sensitive, whereas in our hands both pertussis toxin and cholera toxin failed to modify ADP- or ATP-induced $[Ca^{2+}]_i$ responses. Complement fragment C5a stimulates a Ca^{2+} influx in U-937 cells that does not depend on prior Ca^{2+} mobilization and is insensitive to pertussis toxin. However, La^{3+} was not inhibitory in those studies (42). IP_3 and cAMP can be excluded as second messengers. First, cAMP has no direct effect on Ca^{2+} influx. Second, it decreases $[Ca^{2+}]_i$ plateau, but not spike, levels, likely activating a Ca^{2+}-ATPase. Third, the ADP-evoked rise in IP_3 levels itself depends on Ca^{2+} influx. Ca^{2+} entry could also be secondary to the activation of other conductances. A positive link between hyperpolarization and Ca^{2+} influx has been established in mast cells (43) and neutrophils. In our model, ADP but not ATP induced a small hyperpolarization,[4] which could provide the driving force required to support Ca^{2+} entry through the leaky channels documented in Mn^{2+}-quenching experiments. This initial Ca^{2+} entry could activate a phospholipase C, for instance the probably $[Ca^{2+}]_i$-regulated δ isoform (31), which in turn would mobilize IP_3-sensitive Ca^{2+} stores. Conversely, a small production of IP_3 near the membrane by a receptor-activated phospholipase C could account for the Ca^{2+} entry required to support subsequent production of IP_3 stimulated by ADP. Whatever the initial Ca^{2+} entry mechanism, it results in activation of a phospholipase C, a rise in IP_3 levels, and a slow mobilization of Ca^{2+} stores. This signal amplification system also could explain the fact that store-operated Ca^{2+} entry and ADP-induced Ca^{2+} entry are not additive.

Ca^{2+} influx has been reported to be more relevant than Ca^{2+} mobilization to several cellular processes essentially related to secretion or exocytosis (44). Surface expression of the β_2-integrin family of leukocyte adhesion molecules increases in response to the chemoattractant formyl-methionyl-leucyl-phenylalanine, leukotriene B_4, and other phospholipase C activators (45), but maximal increases require Ca^{2+} influx (46). We found that ADP is more effective than ATP in promoting U-937 cell adhesion. In addition, this effect of ADP was more sensitive than that of ATP to a decrease in Ca^{2+} influx. A likely explanation is that ADP-evoked Ca^{2+} influx induces and/or stabilizes the recruitment of an intracellular pool of adhesion molecules to the cell surface.

In conclusion, ADP and ATP activate U-937 cells through distinct signaling pathways, probably involving specific receptors. The fact that ADP was more effective than ATP in adhesion experiments is probably related to sustained Ca^{2+} influx and might be physiologically relevant.

Acknowledgments

We are greatly indebted to Dr. Morlière and his group, F. Gaboriau, and M. Gèze (U312 INSERM) for granting access to the SPEX F-112 spectrofluorometer and to Dr. M. Maratra (Institute de Recherche sur la Sauté et le Mèdicament, Rhône-Poulenc) for access to the ACAS Meridian scanning cytofluorometer. The technical assistance of Mrs. A. Courtalon for cell cultures and IP_3 measurements, Mrs. N. Achaibou for cytofluorometric data acquisition, and Miss N. Merbouh for desensitization studies with quartz slides is gratefully aknowledged. Western blot analysis was kindly performed by Dr. M. Camps (German Cancer Research Center, Heidelberg, Germany). We also thank Drs. F. Pecker and J. Hanoune for critical reading of the manuscript and Dr. G. Schultz for fruitful discussion.

References

1. Boyer, J. L., C. P. Downes, and T. K. Harden. Kinetics of activation of phospholipase C by P_{2Y} purinergic receptor agonists and guanine nucleotides. *J. Biol. Chem.* **264**:884–890 (1989).
2. Cowen, D. S., H. M. Lazarus, S. B. Shurin, S. E. Stoll, and G. R. Dubyak. Extracellular adenosine triphosphate activates calcium mobilization in human phagocytic leukocytes and neutrophil/monocyte progenitor cells. *J. Clin. Invest.* **83**:1651–1660 (1989).
3. Gordon, J. L. Extracellular ATP: effects, sources and fates. *Biochem. J.* **233**:309–319 (1986).
4. O'Connor, S. E., I. A. Dainty, and P. Leff. Further subclassification of ATP receptors based on agonist studies. *Trends Pharmacol. Sci.* **12**:137–141 (1991).
5. Cusack, N. J., and S. M. O. Hourani. Subtypes of P_2-purinergic receptors: studies using analogues of ATP. *Ann. N. Y. Acad. Sci.* **603**:172–181 (1990).
6. Beyer, E. C., and T. H. Steinberg. Evidence that the gap junction protein connexin-43 is the ATP-induced pore of mouse macrophages. *J. Biol. Chem.* **266**:7971–7974 (1991).
7. Benham, C. D., and R. W. Tsien. A novel receptor-operated Ca^{2+}-permeable channel activated by ATP in smooth muscle. *Nature (Lond.)* **328**:275–279 (1987).
8. Sage, S. O., and T. J. Rink. Kinetic differences between thrombin-induced and ADP-induced calcium influx and release from internal stores in fura-2-loaded human platelets. *Biochim. Biophys. Res. Commun.* **136**:1124–1129 (1986).
9. Lustig, K. D., A. K. Shiau, A. J. Brake, and D. Julius. Expression cloning of an ATP receptor from mouse neuroblastoma cells. *Proc. Natl. Acad. Sci. USA* **90**:5113–5117 (1993).
10. Webb, T. E., J. Simon, B. J. Krishek, A. N. Bateson, T. G. Smart, B. F. King, G. Burnstock, and E. A. Barnard. Cloning and functional expression of a brain G-protein-coupled ATP receptor. *FEBS Lett.* **324**:219–224 (1993).
11. Proctor, R. A., L. C. Denlinger, P. S. Leventhal, S. K. Daugherty, J.-W. Van de Loo, T. Tanke, G. S. Firestein, and P. J. Bertics. Protection of mice from endotoxic death by 2-methylthio-ATP. *Proc. Natl. Acad. Sci. USA* **91**:6017–6020 (1994).
12. Sakamoto, H., and F. Firkin. Characterization of leukocyte phagocytic stimulatory material released by activated human platelets. *Br. J. Haematol.* **57**:49–60 (1984).

[3] F. Gaboriau and M. A. Ventura, unpublished observations.
[4] F. Gaboriau and M. A. Ventura, unpublished obeservations.

13. Dubyak, G. R., D. S. Cowen, and L. M. Meuller. Activation of inositol phospholipid breakdown in HL-60 cells by P_2-purinergic receptors for extracellular ATP: evidence for mediation by both pertussis toxin-sensitive and pertussis toxin-insensitive mechanisms. *J. Biol. Chem.* **263**:18108–18117 (1988).
14. Pfeilschifter, J., B. Thüring, and F. Festa. Extracellular ATP stimulates poly(inositol phospholipid) hydrolylisis and eicosanoid synthesis in mouse peritoneal macrophages in culture. *Eur. J. Biochem.* **186**:509–513 (1989).
15. Greenberg, S., F. Di Virgilio, T. H. Steinberg, and S. C. Silverstein. Extracellular nucleotides mediate Ca^{2+} fluxes in J774 macrophages by two distinct mechanisms. *J. Biol. Chem.* **263**:10337–10343 (1988).
16. Altieri, D. C., P. M. Mannucci, and A. M. Capitanio. Binding of fibrinogen to human monocytes. *J. Clin. Invest.* **78**:968–976 (1986).
17. Maudsley, D. J., and A. G. Morris. Rapid intracellular calcium changes in U-937 monocyte cell line: transient increases in response to platelet-activating factor and chemotactic peptide but not interferon-γ or lipopolysaccharide. *Immunology* **61**:189–194 (1987).
18. Pleass, R., N. J. Cusack, and J. Westwick. An ATP receptor that mediates increases in intracellular calcium in U-937 cells is a P_{2y} purinoceptor. *Eur. J. Pharmacol.* **183**:1605–1606 (1990).
19. Johnston, R. B. Monocytes and macrophages. *N. Engl. J. Med.* **318**:747–752 (1988).
20. Ventura, M. A., A. Ribier, I. Delbourg, A. M. Chambaut-Guerin, and P. Thomopoulos. The adhesiveness of monocytic U-937 cells is stimulated by pro-inflammatory agents and inhibited by adenosine 3′:5′-cyclic monophosphate. *Biochem. Pharmacol.* **39**:677–683 (1990).
21. Ventura, M. A., and P. Thomopoulos. Effect of ATP and ADP on U-937 promonocyte cell adhesiveness and intracellular Ca^{2+} levels. *Nucleosides Nucleotides* **10**:1195–1197 (1991).
22. Issaad, C., M. A. Ventura, and P. Thomopoulos. Biphasic regulation of macrophage attachment by activators of cyclic adenosine monophosphate-dependent kinase and protein kinase C. *J. Cell. Physiol.* **140**:317–322 (1989).
23. Hernandez-Cruz, A., F. Sala, and P. R. Adams. Subcellular calcium transients visualized by confocal microscopy in a voltage-clamped vertebrate neuron. *Science (Washington D. C.)* **247**:858–862 (1990).
24. Sokal, R. R., and F. J. Rohlf. *Biometry*. W. H. Freeman and Co., San Francisco (1981).
25. IUPHAR. 1994 receptor and ion channel nomenclature supplement, ed. 5. *Trends Pharmacol. Sci.* 38 (1994).
26. Silva, A. M., L. M. Rosario, and R. M. Santos. Background Ca^{2+} influx mediated by a dihydropyridine- and voltage-insensitive channel in pancreatic β-cells. *J. Biol. Chem.* **269**:17095–17103 (1994).
27. Dixon, C. J., N. M. Woods, K. S. R. Cuthberson, and P. H. Cobbold. Evidence for two Ca^{2+}-mobilizing purinoceptors on rat hepatocytes. *Biochem. J.* **269**:499–502 (1990).
28. Frelin, C., J. P. Breittmayer, and P. Vigne. ADP induces inositol phosphate-independent intracellular Ca^{2+} mobilization in brain capillary endothelial cells. *J. Biol. Chem.* **268**:8787–8792 (1993).
29. Leichleiter, J., S. Girard, D. Clapham, and E. Peralta. Subcellular patterns of calcium release determined by G protein-specific residues of muscarinic receptors. *Nature (Lond.)* **350**:505–508 (1991).
30. Offermans, S., T. Wieland, D. Homann, J. Sandmann, E. Bombien, K. Spicher, G. Schultz, and K. H. Jakobs. Transfected muscarinic acetylcholine receptors selectively couple to G_i-type G proteins and $G_{q/11}$. *Mol. Pharmacol.* **45**:890–898 (1994).
31. Exton, J. H. Phosphoinositide phopholipases and G proteins in hormone action. *Annu. Rev. Physiol.* **56**:349–369 (1994).
32. Diliberto, P. A., G. Gordon, and B. Herman. Regional and mechanistic differences in platelet-derived growth factor-isoform-induced alterations in cytosolic free calcium in porcine vascular smooth muscle cells. *J. Biol. Chem.* **266**:12612–12617 (1991).
33. Barnard, E. A., G. Burnstock, and T. A. Webb. G protein-coupled receptors for ATP and other nucleotides: a new receptor family. *Trends Pharmacol. Sci.* **15**:67–70 (1994).
34. Jenkins, A. L., M. D. Bootma, M. J. Berridge, and S. R. Stone. Differences in intracellular calcium signaling after activation of the thrombin receptor by thrombin and agonist peptide in osteoblast-like cells. *J. Biol. Chem.* **269**:17104–17110 (1994).
35. Berridge, M. J., and R. F. Irvine. Inositol phosphates and cell signaling. *Nature (Lond.)* **341**:197–204 (1989).
36. Cooper, C. L., A. J. Morris, and T. K. Harden. Guanine nucleotide-sensitive interaction of a radiolabeled agonist with a phospholipase C-linked P_{2y} purinergic receptor. *J. Biol. Chem.* **264**:6202–6206 (1989).
37. Fasolato, C., B. Innocenti, and T. Pozzan. Receptor-activated Ca^{2+} influx: how many mechanisms for how many channels? *Trends Pharmacol. Sci.* **15**:77–83 (1994).
38. Chow, S. C., G. E. N. Kass, and S. Orrenius. Two independently regulated Ca^{2+} entry mechanisms coexist in Jurkat T cells during T cell receptor antigen activation. *Biochem. J.* **293**:395–398 (1993).
39. Hashimoto, Y., A. Ogihara, S. Nakanishi, Y. Matsuda, K. Kurokawa, and Y. Nonomura. Two thrombin-activated Ca^{2+} channels in human platelets. *J. Biol. Chem.* **267**:17078–17081 (1992).
40. Stephens, L., A. Smrca, F. T. Cooke, T. R. Jackson, P. C. Sternweiss, and P. T. Hawkins. A novel phosphoinositide 3-kinase activity in myeloid-derived cells is activated by G protein $\beta\gamma$ subunits. *Cell* **77**:83–93 (1994).
41. Krautwurst, D., R. Seifert, J. Hescheler, and G. Schultz. Formyl peptides and ATP stimulate Ca^{2+} and Na^+ inward currents through non-selective cation channels via G-proteins in dibutyryl cyclic AMP-differentiated HL-60 cells. *Biochem. J.* **288**:1025–1035 (1992).
42. Monk, P. N., and L. J. Partridge. Characterization of a complement-fragment-C5a-stimulated calcium-influx mechanism in U-937 monocytic cells. *Biochem. J.* **295**:679–684 (1993).
43. Penner, R., G. Matthews, and E. Neher. Regulation of calcium influx by second messengers in rat mast cells. *Nature (Lond.)* **334**:499–504 (1988).
44. Kim, K. T., and E. W. Westhead. Cellular responses to Ca^{2+} from extracellular and intracellular sources are different as shown by simultaneous measurements of cytosolic Ca^{2+} and secretion from bovine chromaffin cells. *Proc. Natl. Acad. Sci. USA* **86**:9881–9885 (1989).
45. Miller, L. J., D. F. Bainton, N. Borregaard, and T. A. Springer. Stimulated mobilization of monocyte Mac-1 and p150,95 adhesion proteins from an intracellular vesicular compartment to the cell surface. *J. Clin. Invest.* **80**:535–544 (1987).
46. Berger, M., D. L. Birk, E. M. Wetzler, J. J. O'Shea, E. J. Brown, and A. S. Cross. Calcium requirements for increased complement receptor expression during neutrophil activation. *J. Immunol.* **135**:1342–1348 (1985).

Send reprint requests to: M. A. Ventura, U 282 INSERM, Hôpital Henri Mondor, 94010 Créteil, France.